EFFICIENT MODELING OF CONTINUUM BLADES USING ANCF CURVED SHELL ELEMENT

Ayman A. Nada

College of Engineering, Jazan University, Jazan-442502, KSA.
anada@jazanu.edu.sa

Key words: Wind Turbine Blade, Continuum Mechanics, Plate and Shell elements.

Abstract.   Large-size wind turbine blade is divided into two regions classified by structural and aerodynamic characteristics. The structural region (blade-root section), carries the highest load with low aerodynamics efficiency. The aerodynamical region (blade-span), is aerodynamically significant and therefore thinnest finite element can be utilized. Recently, the Absolute Nodal Coordinate Formulation (ANCF) is used for constructing continuum models of blade-span with uniform structure. Furthermore, a non-uniform and twisted structure model is constructed successfully. These models utilized the ANCF thin plate element due to its aerodynamical nature. However, it is concluded that the use of thin plate element, specifically in the structural region, is not the optimum choice due to the ignorance of the strain along the element thickness. Furthermore, it is found in that the use of thick plate element within the ANCF leads to high numerical stiffness because of the oscillation of gradient along the element thickness. In this investigation, a modified displacement field is used such that a material point is defined by the midsurface and the rotation of the element fiber along the material line. This line is orthogonal to the midsurface in the undeformed configuration. The strain vector is formalized, taking into consideration, the membrane as well as curvature strain. Numerical methods are carried out to estimate the elastic forces and the generalized force Jacobian. The static solution of 40[m] long is carried out using NR method successfully. It is concluded that the use of shell element can be enhance the dynamic model for design process of such blades.

1   INTRODUCTION

The ANCF is designed for large deformation problems in multibody systems applications. In the ANCF, the global position vector gradients are introduced as nodal coordinates in order to model rotation and deformation field of an infinitesimal volume within the element [1]. Only the vectorial quantities that include the global position vector and the position vector gradients are interpolated [2]. As a result, a non-incremental procedures which are implemented in the general multibody dynamics computer algorithms,

can be employed for solving the equations of motion. Furthermore, due to the use of slope coordinates introduced for parameterizing the element rotation and deformation fields, this formulation leads to a constant mass matrix. This, in turn, simplifies the description for the equations of motion since the quadratic velocity vector becomes identically equal to zero [1, 3]. In contrast, the use of a global coordinate system for the definitions of the nodal coordinates leads to a nonlinear expression for the elastic forces.

A sub-family of beam, plate and cable finite elements with large deformations are proposed and employed the 3D theory of continuum mechanics [1]. The development of plate elements based on the ANCF can be categorized into two groups. In the first group, the transverse shear deformation is assumed to be insignificant, allowing the plate elements to be described with position coordinates and slope vectors in a surface direction [4]. This leads to a kinematic description in which the element is defined by the midsurface. In the second group of plate elements, transverse shear deformation is captured by introducing additional slopes in the element transverse direction [5].

In the case of modeling large-size wind turbine blade, the blade is divided into two regions classified by structural and aerodynamic characteristics. The structural region (blade-root section), carries the highest load with low aerodynamics efficiency. The aerodynamical region (blade-span), is aerodynamically significant and therefore thinnest finite element can be utilized. The ANCF is used for constructing continuum models of blade-span with uniform structure [6]. Furthermore, a non-uniform and twisted structure model is carried out in [7]. Both models utilized the ANCF thin plate element due to its aerodynamical nature. The complete blade model with its two regions as well as methods of modeling slope discontinuities are carried out in [8] successfully. However, it is concluded that the use of thin plate element, specifically in the structural region, is not the optimum choice due to the ignorance of the strain along the element thickness. Furthermore, it is found in that the use of thick plate element within the ANCF leads to high numerical stiffness because of the oscillation of gradient along the element thickness. In this investigation, the modified displacement field [9], is used such that a material point is defined by the midsurface and the rotation of the element fiber along the material line, that is orthogonal to the midsurface in the undeformed configuration. Such material line remains straight and unstretched during the deformations. It is considered that the material line in the direction of normal vector at the curvilinear coordinate system. Therefore, the strain of initially curved shell element can be represented as the difference between the current and initial values. In this investigation, by using this displacement filed, the strain vector is formalized, taking into consideration, the membrane as well as curvature strain. The numerical methods are carried out to estimate the elastic forces and the generalized force Jacobian. The static solution of 40[m] long is carried out using NR method successfully and the results and concluded remarks are discussed in the last section.

2   ABSOLUTE NODAL COORDINATE FORMULATION

In the absolute nodal coordinate formulation, the nodal coordinates of the elements are defined in a fixed inertial coordinate system, this fixed inertial coordinate system should be mentioned here as the Structure Coordinate System **SCS:**(XYZ). The nodal coordinates of an element j are consisting of the global displacements and slopes of each node. For a 4-noded thin-plate element, element j, on body i, as shown in Fig.1, the nodal coordinates of node k, $k = (1, 2, 3, 4)$ can be written as:

$$\mathbf{e}^{ijk} = \begin{bmatrix} \mathbf{r}^{ijkT} & \frac{\partial \mathbf{r}^{ijk}}{\partial x^{ij}}^{T} & \frac{\partial \mathbf{r}^{ijk}}{\partial y^{ij}}^{T} \end{bmatrix}^{T} \tag{1}$$

where $\mathbf{r}^{ijk}$ defines the global position of node k and the three vectors $\partial \mathbf{r}^{ijk}/\partial x^{ij}$, and $\partial \mathbf{r}^{ijk}/\partial y^{ij}$, define the position vector gradients at node k with respect to the element coordinate system **ECS**. As a consequence, such a representation guarantees inter-element continuity of global displacement gradients at these points. The nodal coordinates of one element can then be given by the vector $\mathbf{e}^{ij} = \begin{bmatrix} \mathbf{e}^{ij1T} & \mathbf{e}^{ij2T} & \mathbf{e}^{ij3T} & \mathbf{e}^{ij4T} \end{bmatrix}^{T}$. In the ANCF, the global position of an arbitrary point on the mid-surface of body i, element j, is defined as:

$$\mathbf{r}_m^{ij} = \mathbf{S}^{ij} \left(\mathbf{u}^{ij} \right) \mathbf{e}^{ij} \tag{2}$$

where $\mathbf{S}^{ij}$ is the element shape function matrix, $\mathbf{u}^{ij} = \begin{bmatrix} x^{ij} & y^{ij} \end{bmatrix}^{T}$ is the local position of the point, x^{ij}, and y^{ij} are the local coordinates of the element defined in the **ECS.** By defining $\mathbf{p}^i$ as the *unconstrained* vector of nodal coordinates over the flexible body i, with the dimension of $DOFs \times 1$, where $DOFs$ are the total number of degrees of freedom. Thus, Eqn.(2) can be rewritten as:

$$\mathbf{r}_m^{ij} = \mathbf{S}^{ij} \mathbf{e}^{ij} = \mathbf{S}^{ij} \mathbf{B}_1^{ij} \mathbf{B}_2^i \mathbf{p}^i \tag{3}$$

where $\mathbf{B}_1^{ij}$ is the connectivity matrix and $\mathbf{B}_2^i$ is boundary conditions linear-transformation matrix.

The kinematic representation of shell models are usually pertain to the admissible displacement profile through the shell thickness. In this investigation, the assumptions connect the displacements of points located on a material line that is orthogonal to the midsurface in the undeformed configuration. More specifically, it is usually assumed (and experimentally substantiated) that any such material line remains straight and unstretched during the deformations, see Fig. (1) which is expressed by the following equation:

$$\mathbf{r} = \mathbf{S}\mathbf{e} + z\,\mathbf{n} = \mathbf{r}_m + z\,\mathbf{n} \tag{4}$$

in which, the superscript notation ij is removed for simplicity. In this equation, it is considered that the material line in the direction of $\mathbf{n}$ at the curvilinear coordinate system
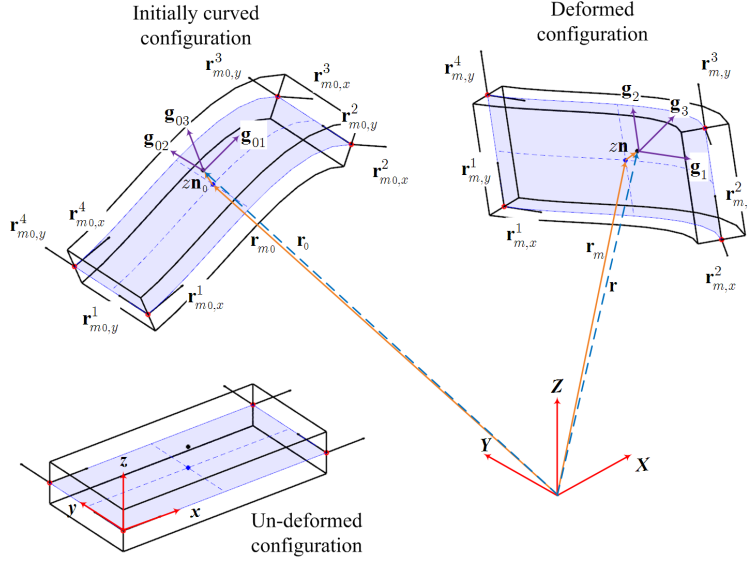
Figure 1: Kinematic representation of curved plate element

$(\mathbf{g}_1, \mathbf{g}_2)$. The normal vector $\mathbf{n}$ of the mid-surface of the plate is defined using cross product of the vectors $\mathbf{r}_x$ and $\mathbf{r}_y$, with subscript x and y refer to partial derivatives with respect to these coordinates. The displacement $\mathbf{r}_m$ represents a global displacement of the an arbitrary point along the mid-surface. The displacement $z\,\mathbf{n}$ is due to the rotation of the line. It should be noted that the rotation of an infinitely-thin straight material line is uniquely defined by a rotation vector normal to that mid-surface. The gradient vectors of the deformed shape can be represented as:

$$
\begin{aligned}
\mathbf{g}_1 &= \frac{\partial \mathbf{r}}{\partial x} = \frac{\partial \mathbf{r}_m}{\partial x} + z\,\frac{\partial \mathbf{n}}{\partial x} \\
\mathbf{g}_2 &= \frac{\partial \mathbf{r}}{\partial y} = \frac{\partial \mathbf{r}_m}{\partial x} + z\,\frac{\partial \mathbf{n}}{\partial x} \\
\mathbf{g}_3 &= \frac{\partial \mathbf{r}}{\partial z} = \mathbf{n} = \frac{\mathbf{g}_1 \times \mathbf{g}_2}{\|\mathbf{g}_1 \times \mathbf{g}_2\|}
\end{aligned}
\tag{5}
$$

The position vector of the an arbitrary point lies on the shell element in the initially curved configuration, can be represented by the position vector of the point along the mid-surface and normal vector as follows:

$$
\left.
\begin{aligned}
\mathbf{r}_0 &= \mathbf{r}_{m0} + z\,\mathbf{n}_0\,(\mathbf{u}) \\
\mathbf{r}_{m0} &= \mathbf{S}\mathbf{e}_0
\end{aligned}
\right\}
\tag{6}
$$

where the subsrcipts m and 0 are referring to the mid-surface and initial configuration, respectively. The local curved surface coordinate frame for the undeformed configuration
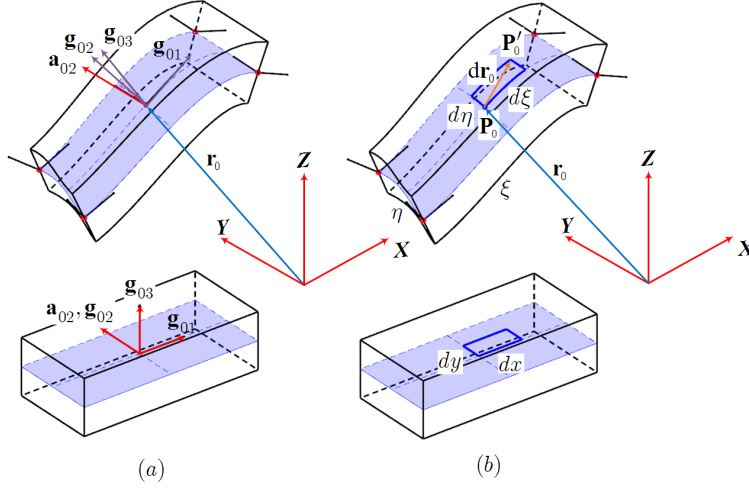
4

Figure 2: Strain measure of mid-surface plane of initially curved confiduration

can be represented by the tripad $(\mathbf{g}_{01}, \mathbf{g}_{02}, \mathbf{n}_0)$. Since the gradient vectors $\mathbf{r}_{m0x}$ and $\mathbf{r}_{m0y}$ are not orthogonal, see Fig.(2), and therefore, the curved-surface frame $(\mathbf{g}_{m01}, \mathbf{g}_{m02}, \mathbf{n}_{m0})$ does not represent a Cartesian frame, which is generally can not be correlated by the constitutive equations. The Cartesian coordinate frame $(\mathbf{a}_{m01}, \mathbf{a}_{m02}, \mathbf{a}_{m03})$ can be defined as:

$$\left. \begin{aligned} \mathbf{a}_{m01} &= \mathbf{g}_{m01} \\ \mathbf{a}_{m02} &= \mathbf{a}_{m03} \times \mathbf{a}_{m01} \\ \mathbf{a}_{m03} &= \mathbf{n}_{m0} \end{aligned} \right\} \tag{7}$$

The relationship between these two local coordinates can be found as:

$$\begin{bmatrix} d\xi \\ d\eta \end{bmatrix} = \begin{bmatrix} a\left(\mathbf{g}_{m01} \cdot \mathbf{a}_{m01}\right) & a\left(\mathbf{g}_{m01} \cdot \mathbf{a}_{m02}\right) \\ b\left(\mathbf{g}_{m02} \cdot \mathbf{a}_{m01}\right) & b\left(\mathbf{g}_{m02} \cdot \mathbf{a}_{m02}\right) \end{bmatrix}^{-T} \begin{bmatrix} dx \\ dy \end{bmatrix} = \mathbf{J} \begin{bmatrix} dx \\ dy \end{bmatrix} \tag{8}$$

where a and b are the length and width of the plate elements, respectively. Since $\mathbf{g}_{m01} \cdot \mathbf{a}_{m02} = 0$, the transformation matrix can be written as:

$$\mathbf{J} = \begin{bmatrix} J_{11} & J_{12} \\ 0 & J_{22} \end{bmatrix} = \begin{bmatrix} 1/a & J_{12} \\ 0 & J_{22} \end{bmatrix} \tag{9}$$

2.1 Membrane strain of initially curved shell element

Let us assume the point $\mathbf{P}(\xi, \eta)$ is initially located at $\grave{\mathbf{P}}(\xi + d\xi, \eta + d\eta)$ on the mid-surface of the shell element. The infinitesimal arc length $d\mathbf{r}_{m0}$ on the mid-surface can be calculated using the local curved surface coordinate frame as:

$$d\mathbf{r}_{m0} = \mathbf{g}_{m01}d\xi + \mathbf{g}_{m02}d\eta \tag{10}$$

5

where $\mathbf{g}_{m01} = \partial\mathbf{r}_{m0}/\partial x$, $\mathbf{g}_{m02} = \partial\mathbf{r}_{m0}/\partial y$ are the position vector gradients at the mid-surface. The square of arc length, $|dr_{m0}|$, of an infinitesimal segment along the mid-surface of the initially curved element can be approximated by:

$$
\begin{aligned}
|dr_{m0}|^2 &= d\mathbf{r}_{m0} \cdot d\mathbf{r}_{m0} \\
&= (\mathbf{g}_{m01}d\xi + \mathbf{g}_{m02}d\eta) \cdot (\mathbf{g}_{m01}d\xi + \mathbf{g}_{m02}d\eta) \\
&= \begin{bmatrix} d\xi & d\eta \end{bmatrix} \begin{bmatrix} \mathbf{g}_{m01}^T\mathbf{g}_{m01} & \mathbf{g}_{m01}^T\mathbf{g}_{m02} \\ \mathbf{g}_{m01}^T\mathbf{g}_{m02} & \mathbf{g}_{m02}^T\mathbf{g}_{m02} \end{bmatrix} \begin{bmatrix} d\xi \\ d\eta \end{bmatrix}
\end{aligned}
\tag{11}
$$

Therefore, the Green-Lagrange strain of the mid-surface of the shell element can be written as:

$$
\epsilon_0^m = \frac{1}{2}\mathbf{J}^T \begin{bmatrix} \mathbf{g}_{m01}^T\mathbf{g}_{m01} & \mathbf{g}_{m01}^T\mathbf{g}_{m02} \\ \mathbf{g}_{m01}^T\mathbf{g}_{m02} & \mathbf{g}_{m02}^T\mathbf{g}_{m02} \end{bmatrix} \mathbf{J}
\tag{12}
$$

Similarly, in the current (deformed) configuration, the square of arc length, $|dr_m|$, of an infinitesimal segment along the mid-surface takes the form as:

$$
|dr_m|^2 = \begin{bmatrix} d\xi & d\eta \end{bmatrix} \begin{bmatrix} \mathbf{g}_{m1}^T\mathbf{g}_{m1} & \mathbf{g}_{m1}^T\mathbf{g}_{m2} \\ \mathbf{g}_{m1}^T\mathbf{g}_{m2} & \mathbf{g}_{m2}^T\mathbf{g}_{m2} \end{bmatrix} \begin{bmatrix} d\xi \\ d\eta \end{bmatrix}
\tag{13}
$$

The enlongation can be estimated as $(dr_{m0})^2 - (dr_m)^2$, and therefore, membrane strain of the mid-surface at current configuration, ϵ_c^m, can be expressed as::

$$
\begin{aligned}
\epsilon_c^m &= \frac{1}{2}\mathbf{J}^T \left(\begin{bmatrix} \mathbf{g}_{m1}^T\mathbf{g}_{m1} & \mathbf{g}_{m1}^T\mathbf{g}_{m2} \\ \mathbf{g}_{m1}^T\mathbf{g}_{m2} & \mathbf{g}_{m2}^T\mathbf{g}_{m2} \end{bmatrix} - \begin{bmatrix} \mathbf{g}_{m01}^T\mathbf{g}_{m01} & \mathbf{g}_{m01}^T\mathbf{g}_{m02} \\ \mathbf{g}_{m01}^T\mathbf{g}_{m02} & \mathbf{g}_{m02}^T\mathbf{g}_{m02} \end{bmatrix} \right) \mathbf{J} \\
&= \begin{bmatrix} J_{11}^2\epsilon_{11}^m & J_{11}\left(\epsilon_{11}^m J_{12} + \epsilon_{12}^m J_{22}\right) \\ J_{11}\left(\epsilon_{11}^m J_{12} + \epsilon_{12}^m J_{22}\right) & J_{12}\left(\epsilon_{11}^m J_{12} + \epsilon_{12}^m J_{22}\right) + J_{22}\left(\epsilon_{12}^m J_{12} + \epsilon_{22}^m J_{22}\right) \end{bmatrix}
\end{aligned}
\tag{14}
$$

Therefore, the strain vector $\epsilon_c^m = \begin{bmatrix} \epsilon_{c11}^m & \epsilon_{c22}^m & 2\epsilon_{c12}^m \end{bmatrix}^T$ can be formulized as:

$$
\begin{aligned}
\epsilon_{c11}^m &= J_{11}^2\epsilon_{11}^m \\
\epsilon_{c22}^m &= J_{12}\left(\epsilon_{11}^m J_{12} + \epsilon_{12}^m J_{22}\right) + J_{22}\left(\epsilon_{12}^m J_{12} + \epsilon_{22}^m J_{22}\right) \\
\epsilon_{c12}^m &= J_{11}\left(\epsilon_{11}^m J_{12} + \epsilon_{12}^m J_{22}\right)
\end{aligned}
\tag{15}
$$

where

$$
\begin{aligned}
\epsilon_{11}^m &= \mathbf{g}_{m1}^T\mathbf{g}_{m1} - \mathbf{g}_{m01}^T\mathbf{g}_{m01} \\
\epsilon_{22}^m &= \mathbf{g}_{m2}^T\mathbf{g}_{m2} - \mathbf{g}_{m02}^T\mathbf{g}_{m02} \\
\epsilon_{12}^m &= \mathbf{g}_{m1}^T\mathbf{g}_{m2} - \mathbf{g}_{m01}^T\mathbf{g}_{m02}
\end{aligned}
\tag{16}
$$

where ε_{xx} and ε_{yy} are the normal strain components in x and y direction and ε_{xy} is the shear strain.

2.2 Curvature strain of initially curved shell element

Recalling the position vector of an arbitrary point along the deformed shape, Eq.(4); where $\mathbf{r}_m$ is the vector that defines the mid-surface of the plate, and $z\,\mathbf{n}$ is the vector that defines a fiber of the plate. The curvature strain ε^κ, of initially curved element can be given by the following equation:

$$\varepsilon^\kappa_c = z\mathbf{J}^T\left(\kappa - \kappa_0\right)\mathbf{J} \tag{17}$$

This equation, Eq. (17) can be written explicitly as:

$$
\begin{aligned}
\varepsilon^\kappa_c &= z\mathbf{J}^T \begin{bmatrix} \kappa_{11} - \kappa_{011} & \kappa_{12} - \kappa_{012} \\ \kappa_{12} - \kappa_{012} & \kappa_{22} - \kappa_{022} \end{bmatrix} \mathbf{J} \\
&= z \begin{bmatrix} J_{11}^2 \kappa_{c11} & J_{11}\left(J_{12}\kappa_{c11} + J_{22}\kappa_{c12}\right) \\ J_{11}\left(J_{12}\kappa_{c11} + J_{22}\kappa_{c12}\right) & J_{12}\left(J_{12}\kappa_{c11} + J_{22}\kappa_{c12}\right) + J_{22}\left(J_{12}\kappa_{c12} + J_{22}\kappa_{c22}\right) \end{bmatrix}
\end{aligned} \tag{18}
$$

Therefore, the strain vector $\epsilon^\kappa_c = \begin{bmatrix} \epsilon^\kappa_{c11} & \epsilon^\kappa_{c22} & 2\epsilon^\kappa_{c12} \end{bmatrix}^T$ can be formulized as:

$$
\begin{aligned}
\epsilon^\kappa_{c11} &= J_{11}^2 \kappa_{c11} \\
\epsilon^\kappa_{c22} &= J_{12}\left(\kappa_{c11}J_{12} + \kappa_{c12}J_{22}\right) + J_{22}\left(\kappa_{c12}J_{12} + \kappa_{c22}J_{22}\right) \\
\epsilon^\kappa_{c12} &= J_{11}\left(J_{12}\kappa_{c11} + J_{22}\kappa_{c12}\right)
\end{aligned} \tag{19}
$$

such that, the curvature components can be evaluated as:

$$
\begin{aligned}
\kappa_{c11} &= \kappa_{11} - \kappa_{011} = \mathbf{n}^T\mathbf{g}_{11} - \mathbf{n}_0^T\mathbf{g}_{011} \\
\kappa_{c22} &= \kappa_{22} - \kappa_{022} = \mathbf{n}^T\mathbf{g}_{22} - \mathbf{n}_0^T\mathbf{g}_{022} \\
\kappa_{c12} &= \kappa_{12} - \kappa_{012} = \mathbf{n}^T\mathbf{g}_{12} - \mathbf{n}_0^T\mathbf{g}_{012}
\end{aligned} \tag{20}
$$

where

$$
\begin{aligned}
\mathbf{g}_{11} &= \frac{\partial^2\mathbf{r}}{\partial x^2} = \frac{\partial^2\mathbf{r}_m}{\partial x^2} + z\,\frac{\partial^2\mathbf{n}}{\partial x^2} \\
\mathbf{g}_{22} &= \frac{\partial^2\mathbf{r}}{\partial y^2} = \frac{\partial^2\mathbf{r}_m}{\partial y^2} + z\,\frac{\partial^2\mathbf{n}}{\partial y^2} \\
\mathbf{g}_{12} &= \frac{\partial^2\mathbf{r}}{\partial x\partial y} = \frac{\partial^2\mathbf{r}_m}{\partial x\partial y} + z\,\frac{\partial^2\mathbf{n}}{\partial x\partial y}
\end{aligned} \tag{21}
$$

2.3 Elastic Forces

Elastic forces within the plate elements based on the ANCF can be obtained by individually treating the in-plane membrane and curvature strain components. The strain energy can be written as the sum of two terms: one term is due to membrane and shear deformations at the plate mid-surface, whereas the other term is due to the plate bending and twist. The strain energy can then be written as follows [1, **?**]:

$$U_e = U_e^m + U_e^\kappa = \frac{1}{2} \int_{V_0} \varepsilon^{m^T} \mathbf{c}^E \varepsilon^m |\mathbf{J}| dV + \frac{1}{2} \int_{V_0} \varepsilon^{\kappa^T} \mathbf{c}^E \varepsilon^\kappa |\mathbf{J}| dV \tag{22}$$

The energy expression given by Eq.(22) is computationally expensive since numerical integration over the element volume is involved. Once the strain energy is calculated, the elastic forces and their Jacobian matrix, called tangential stiffness matrix,can be derived as follows:

$$\mathbf{Q}_e = \mathbf{Q}_e^m + \mathbf{Q}_e^\kappa = \frac{\partial U_e^m}{\partial \mathbf{e}} + \frac{\partial U_e^\kappa}{\partial \mathbf{e}} \tag{23}$$

$$\mathbf{K} = \frac{\partial \mathbf{Q}_e}{\partial \mathbf{e}} \tag{24}$$

In this study, tangential stiffness matrix, **K,** is evaluated numerical by allowing a small perturbations in the nodal coordinates **e** and re-calculating the elastic force $\mathbf{Q}_e$, to find the matrix **K.** The convergence criterion for the iteration is defined such that Euclidean norm of the elastic force vector obey some extent.

3 BLADE MODEL

In the case of modeling span-wise slope discontinuity, lofted surface is constructed along the blade length, particularly between the 'start' and the 'tip' cross and between the 'start' and 'root' sectional curves [8]. In the case of obtaining the global position vector for the non-uniform wind turbine blade; the position vector **r** should be linearly interpolated between the blade starting-chord, c_1, and tip-chord c_2. This bounded curves can be denoted by $\mathbf{r}(\xi, 0)$ and $\mathbf{r}(\xi, 1)$ and by two straight segments $\mathbf{r}(0, \eta)$ and $\mathbf{r}(1, \eta)$ connecting them. Surface lines in η direction are therefore straight,i.e., lofted surfaces [**?**], whereas each line in the ξ direction is a blend of $\mathbf{r}(\xi, 0)$ and $\mathbf{r}(\xi, 1)$ this blend constitutes the surface expression of:

$$\mathbf{r}(\xi, \eta) = (1 - \eta)\mathbf{r}(\xi, 0) + \eta\,\mathbf{r}(\xi, 1) \tag{25}$$

where η and ξ are parametric domains such that $\xi, \eta \in [0, 1]$ and can be estimated as $\xi = x/a, \eta = y/b$, with a, and b are the element length and width respectively. It should be mentioned here that this kind of surface is fully defined by specifying the two boundary curves. Similar procedure can be carried out to construct the blade-root section. The start

cross section of the blade is used with the circular edge of the root surface to construct the lofting surface between them. The boundary curves can be written as:

$$\mathbf{r}(\xi, 0) = \mathbf{r}^i = \mathbf{S}(x, 0)\,\mathbf{e} \quad \cdots, x \in [0, c_1] \tag{26}$$

where $\mathbf{e}$ is the nodal coordinates along the curve of the starting-chord, curve i. Thus, the position vector of an arbitrary point along the tip curve, curve j, can be concluded as:

$$\mathbf{r}(\xi, 1) = \mathbf{r}^j = \begin{bmatrix} 0 \\ L_s \\ 0 \end{bmatrix} + \begin{bmatrix} \frac{c_2}{c_1} & 0 & 0 \\ 0 & 1 & 0 \\ 0 & 0 & \frac{c_2}{c_1} \end{bmatrix} \mathbf{r}(\xi, 0) \cdots, x \in [0, c_2] \tag{27}$$

whereas the position vector of an arbitrary point along the circular root curve, curve k, can be obtained as:

$$\mathbf{r}(\xi, 1) = \mathbf{r}^k = \begin{bmatrix} 0 \\ -L_r \\ 0 \end{bmatrix} + \begin{bmatrix} \cos\theta & 0 & 0 \\ 0 & 0 & 0 \\ 0 & 0 & \sin\theta \end{bmatrix} c_r \cdots, \theta \in [0, 2\pi] \tag{28}$$

such that c_1, c_2, c_r are the chord lengths at the starting, tip and root sections along the blade. simply c_r is the radius of the circular curve of the blade-root. L_s and L_r are the blade-span and blade-root lengths, such that the total length of the blade is $L_s + L_r$. By substituting Eq.(26 , 27) into Eq.(25) gives the lofted surfaces between $\mathbf{r}^i$ and $\mathbf{r}^j$, which can be solved for the nodal positions at the tip curve. Also, By substituting Eq.(26 , 28) into Eq.(25) gives the lofted surfaces between $\mathbf{r}^i$ and $\mathbf{r}^k$, which can be solved for the nodal positions at the circular root curve, see Fig.(3). The span-wise slope discontinuity can be modeled by using the lofting equation for the gradients transformation as well as the nodal position transformation. The gradients of the lofted surface can be obtained as:

$$\frac{d\mathbf{r}(\xi, \eta)}{d\xi} = (1 - \eta)\frac{d\mathbf{S}(\xi, 0)}{d\xi}\mathbf{e} + \eta\frac{d\mathbf{S}(\xi, 1)}{d\xi}\mathbf{e} \tag{29}$$

$$\frac{d\mathbf{r}(\xi, \eta)}{d\eta} = -\mathbf{r}(\xi, 0) + \mathbf{r}(\xi, 1) \tag{30}$$

It is therefore, available to obtain the nodal positions and gradients necessary to construct the ANCF model of a complete blade structure for the blade-span section as well as for the blade-root section. It is necessary to emphasis that using Eq.(29, 30), a continuous ANCF model can be obtained for the structure of large-size wind turbine blade.

The performance of the curved shell element based on the rotation of the fiber line is studied through static test, in which, the blade is fixed at its root side while the structure is subjected to a force of 2, 5 and 10 KN acting at its tip, see Fig. (5). The blade specifications are as follows: NACA 4412 profile, blade-span length $L_s = 30\,[m]$, blade-root length $L_r = 10\,[m]$, root radius $c_r = 1\,[m]$, taper angle of 5°, twist angle of 5°, chord
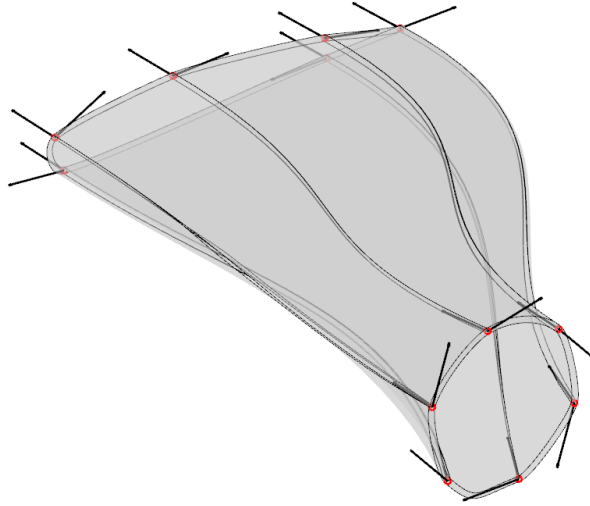
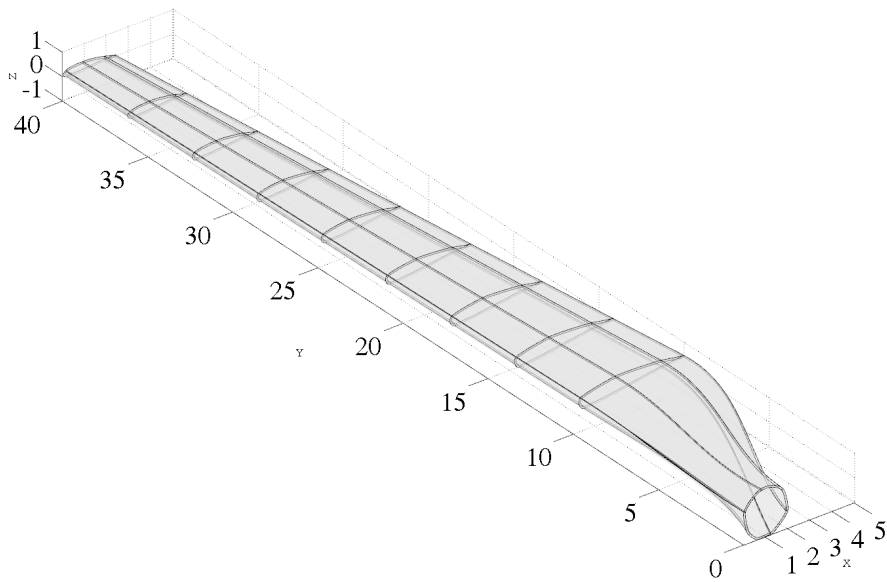**Figure 3**: ANCF model of blade-root section using curved shell elements

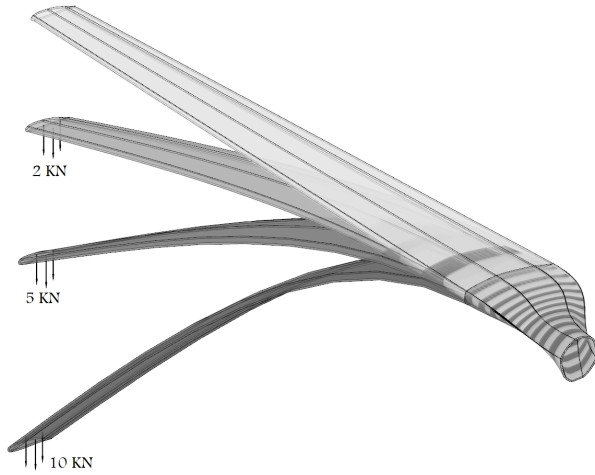**Figure 4**: 40 [m] wind turbine blade with multi-sectional along the blade span (8-sections)

Figure 5: Static Deflection of large-size blade
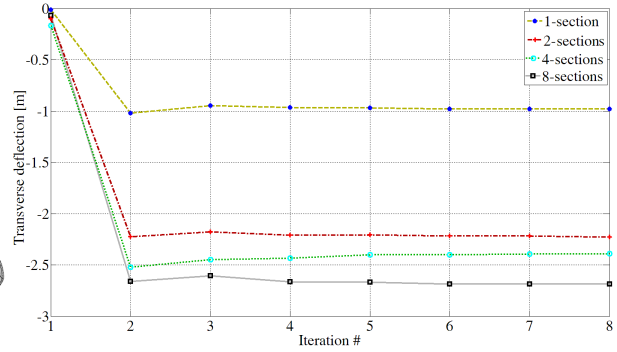

Figure 6: Numerical convergence and accuracy

length at the blade start-section $c_1 = 5\,[m]$. The static solution is convergent mostly at the third iteration, see Fig.(6), however, it is clearly seen that the blade model of lower elements performs poorly and it is not able to capture the accurate solution, in Fig.(6), each section include 6 elements.

4   CONCLUSION

In modeling large-size wind turbine blades; the use of thick plate description may lead to curve-induced distortion and, consequently, membrane locking associated with strain components along x-axis and y-axis. It is also known that the strain component along z-axis leads to curvature thickness locking. However, it is concluded that the use of thin plate element, specifically in the structural region, is not the optimum choice due to the ignorance of the strain along the element thickness. This paper introduce the blade model with a modified displacement filed in order to take the curved nature as well as the considerable thickness into consideration. In this displacement field, a material point is defined by the midsurface and the rotation of the element fiber along the material line. This line is orthogonal to the midsurface in the undeformed configuration. Numerical methods are carried out to estimate the elastic forces and static solution of 40[m] long blade subjected to static loads is carried out using Newton-Raphson method successfully. It is concluded that the number of blade-sections, i.e., number of elements along the blade span, is playing an important role in the solution accuracy.

REFERENCES

[1] Shabana, A.A., 2010, *Computational Continuum Mechanics*, Cambridge University press,Cambridge, UK.

[2] Gerstmayr, J., Sugiyama, H., Mikkola, A., 2013," Review on the Absolute Nodal Co-

ordinate Formulation for Large Deformation Analysis of Multibody Systems", Journal of Computational and Nonlinear Dynamics, 2013 8(3):031016.

[3] Sugiyama,H., Escalona, J., and Shabana, A.A., 2003, "Formulation of Three-Dimensional Joint Constraints Using the Absolute Nodal Coordinates. Nonlinear Dynamics", 31:pp.167-195.

[4] Dufva, K. and Shabana, A.A., 2005. "Analysis of Thin Plate Structure Using the Absolute Nodal Coordinate Formulation, IMechE Journal of Multi-body Dynamics", 219, PP:345-355.

[5] Mikkola, A. M. and Shabana, A. A.: A non-incremental finite element procedure for the analysis of large deformation of plates and shells in mechanical system applications. Multibody Syst. Dyn., 2003, 9(3), 283–309.

[6] Nada, Ayman A., 2013, "Use of B-spline Surface to Model Large-Deformation Continuum Plates: Procedure and Applications", Nonlinear dynamics, 72, pp 243-263.

[7] Bayoumy, A.H., Nada, A.A., Megahed, S.M., 2013, "A Continuum Based Three-Dimensional Modeling of Wind Turbine Blades", Comput. Non. Dyn., 8(3).

[8] Bayoumy, A.H., Nada, A.A., Megahed, S.M., "Modeling Slope Discontinuity Of Large Size Wind-Turbine Blade Using Absolute Nodal Coordinate Formulation", ASME(IDETC/CIE 2012), Chicago, Illinois, USA.

[9] Yan, D. et.al., 2013, "A new curved gradient deficient shell element of absolute nodal coordinate formulation for modeling thin shell structures", Nonlinear Dyn., 74(1-2).